Original Article

A putative SUBTILISIN-LIKE SERINE PROTEASE 1 (SUBSrP1) regulates anther cuticle biosynthesis and panicle development in rice

Asif Ali [a], Tingkai Wu [a], Hongyu Zhang [a], Peizhou Xu [a], Syed Adeel Zafar [b], Yongxiang Liao [a], Xiaoqiong Chen [a], Hao Zhou [a], Yutong Liu [a], Wenming Wang [a,*], Xianjun Wu [a,*]

[a] State Key Laboratory of Crop Gene Exploration and Utilization in Southwest China, Rice Research Institute, Sichuan Agricultural University, Chengdu 611130, China
[b] Department of Botany and Plant Sciences, University of California, Riverside, CA 92521, USA

HIGHLIGHTS

OsSUBSrP1 regulates anther cuticle biosynthesis. *OsSUBSrP1* is essential for apical spikelet development. *OsSUBSrP1* plays an important role in maintaining ROS-mediated programmed cell death.

GRAPHICAL ABSTRACT
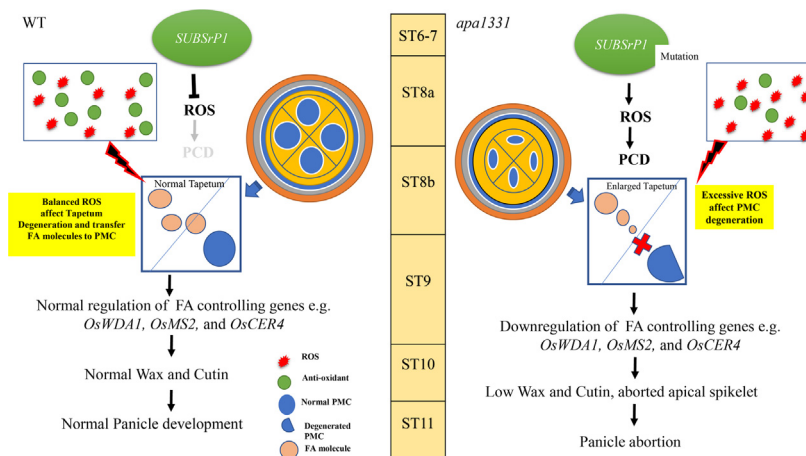
ARTICLE INFO

ABSTRACT

Introduction: Panicle abortion is a severe physiological defect and causes a reduction in grain yield.
Objectives: In this study, we aim to provide the characterization and functional analysis of a mutant *apa1331* (*apical panicle abortion1331*).
Methods: The isolated mutant from an EMS-mutagenized population was subjected to SSR analysis and Mutmap assay for candidate gene mapping. We performed phenotypic analysis, anthers cross-sections morphology, wax and cutin profiling, biochemical assays and phylogenetic analysis for characterization and evaluation of *apa1331*. We used CRISPR/Cas9 disruption for functional validation of its candidate gene. Furthermore, comparative RNA-seq and relative expression analysis were performed to get further insights into mechanistic role of the candidate gene.
Results: The anthers from the apical spikelets of *apa1331* were degenerated, pollen-less and showed defects in cuticle formation. Transverse sections of *apa1331* anthers showed defects in post-meiotic microspore development at stage 89. Gas Chromatography showed a significant reduction of wax and cutin in anthers of *apa1331* compared to Wildtype (WT). Quantification of H_2O_2 and MDA has indicated the excessive ROS (reactive oxygen species) in *apa1331*. Trypan blue staining and TUNEL assay revealed cell death and excessive DNA fragmentation in *apa1331*. Map-based cloning and Mutmap analysis revealed that *LOC_Os04g40720*, encoding a putative *SUBTILISIN-LIKE SERINE PROTEASE (OsSUBSrP1)*,

Peer review under responsibility of Cairo University.

* Corresponding authors.
   E-mail addresses: j316wenmingwang@163.com (W. Wang), wuxjsau@126.com (X. Wu).

harbored an SNP (A > G) in *apa1331*. Phenotypic defects were only seen in apical spikelets due to highest expression of *OsSUBSrP1* in upper panicle portion. CRISPR-mediated knock-out lines of *OsSUBSrP1* displayed spikelet abortion comparable to *apa1331*. Global gene expression analysis revealed a significant downregulation of wax and cutin biosynthesis genes.

Conclusions: Our study reports the novel role of SUBSrP1 in anther cuticle biosynthesis by ROS-mediated programmed cell death in rice.

Introduction

The panicle is a reproductive organ in rice, which directly determines the grain yield [1]. Various genetic and environmental factors regulate the spatiotemporal arrangement of a panicle by affecting its reproductive success and developmental decisions [2]. Abortion of spikelets, also called panicle degeneration, is highly detrimental to plants and causes a significant reduction in yield [3–5]. Although, several genetic factors have been reported that control the apical panicle development in rice. Nevertheless, the molecular basis of mechanisms and why abortion remains in the apical portion still needs a comprehensive understanding.

Development of the panicle begins with the transition of juvenile to the reproductive phase. Various changes at these transitions including shoot, inflorescence and branch meristems could bring severe defects to panicle development [6]. *SMALL PANICLE1 (SP1)* controls the length of the panicle by encoding a nitrate transporter of a PEPTIDE TRANSPORTER (PTR) family [7]. Similarly, *ERRECT PANICLE 2 (EP), LAX PANICLE1 (LAX1)* and *LAX2* are reported to involve in the development of axillary and branch meristems formation [8–10]. *ABERRANT PANICLE ORGANIZATION 1 (APO1)* and *APO2* work in the temporal regulation of meristems, which ultimately affect the inflorescence development [11,12]. *SQUAMOSA PROMOTER BINDING PROTEIN LIKE6 (SPL6)* regulates the signaling outputs by repressing an active transducer INOSITOL-REQUIRING ENZYME 1 (IRE1) of cell death and control panicle development. *SPL6* deficient mutant plants revealed hyperactivation of IRE1 and displayed apical panicle abortion [13]. *ALUMINUM ACTIVATED MALATE TRANSPORTER (OsALMT7)* controls the panicle development by transporting malate to the vascular bundles [3]. A mutation in *CALCINEURIN B-LIKE PROTEIN-INTERACTING PROTEIN KINASE 31 (OsCIPK31)* also displayed apical spikelet abortion phenotype [14]. Mutation in *TUTOU1* that encodes a SUPPRESSOR OF CAMP RECEPTOR (SCAR) like protein also exhibited the apical degeneration phenotype due to disorganization of actin [15]. *OsC6* encodes a LIPID TRANSFER PROTEIN (LTP) and is involved in the post-meiotic development of anthers. Plants silenced for *OsC6* displayed the defective development of pollen exine and tapetum [16]. *DEGENERATED PANICLE AND PARTIAL STERILITY 1 (DPS1)* played an important role in anther cuticle development, and *dps1* plants showed an accumulation of ROS (reactive oxygen species) in apical spikelets [5].

During panicle development, abortion of spikelets frequently occurs either at basal or apical portions of the panicle due to unfavorable conditions [17]. Extreme temperature, malnutrition and drought stress have been identified as potential factors promoting panicle degeneration [3,17–20]. ROS are oxidizing agents and cause dynamic injury to various biological events [21]. Impairments in the panicle, heading date, plant height and number of grains are associated with ROS accumulation that causes damage to cellular tissues and machinery [14,15,22]. Unbalanced ROS homeostasis also leads to defects in meiosis and microspore development [23]. Programmed cell death (PCD) is a controlled process involved in rupturing the nuclear membrane, cytoplasmic shrinkage and swelling of the endoplasmic reticulum [24].

Anthers are the male reproductive organs present inside the spikelet and produce pollen grains via meiosis and mitosis [25]. Anthers have four layers; epidermis, endothecium, middle layer and tapetum. Tapetum is the innermost layer, which serves as a source of nutrients and enzymes during microspore development [26]. Tapetum plays a key role in pollen development and seed setting [27]. Normal tapetum development is often associated with a well-developed cuticle, and it protects anthers from external damages. The cuticle is mainly composed of wax and cutin monomers. Any abnormality in cuticle development leads to the impaired tapetum that ultimately causes the failure in the seed setting [28–30]. Several factors affect cuticle development, such as high temperature, excessive accumulation of ROS and imbalance of certain hormones [31–33]. These factors are either controlled by genetic elements or environmental cues. Anther cuticle and walls share several phenolic and lipidic precursors. Wax and cutin play an essential role in pollen mother cell (PMC) development. C16 and C18 and their derivatives are called cutin, constitute the cuticle of anthers [34]. Several genes controlling cuticle and tapetum development have been identified, such as *WAX-DEFICIENT ANTHER1 (WDA1), DPS1, POST-MEIOTIC DEFICIENT ANTHER1 (PDA1), ATP BINDING CASSETTE TRANSPORTER G26 (OsABCG26), NO POLLEN1 (NP1), IRREGULAR POLLEN EXINE1 (IPE1), DEFECTIVE POLLEN WALL2 (DPW2)*, and *DPW3* have been reported to play their role in anther development by regulating wax and cutin pathway [5,35–41]. Similarly, *MALE STERILE2 (MS2)* and *DPW2* play their part in developing pollens by regulating the expression of FATTY ACYL TRANSFERASE [40,42].

The protein family of SUBTILISIN-LIKE SERINE PROTEASE (Subtilisin) is not well studied in plants. However, their role as CASPASES in animals has been widely reported. Subtilisins display a cleavage specificity and have a particular function in PCD [43,44]. Plant subtilisins have been reported to play their role in the processing of peptide growth factors [45], fruit ripening [46], xylem differentiation [47], plant-pathogen recognition [48] and determination of silique number [49]. A few plant studies have also indicated their role in reproductive organs, and a meiotic protein was reported to involve in events of late microsporogenesis [50,51].

The current study is a genetic analysis and functional validation of our previous preliminary study of a gene mapped on chromosome 4 controlling panicle abortion phenotype [52]. We presented a novel function of a putative *OsSUBSrP1,* which is essential for anther cuticle formation and panicle development. An ethyl methane-sulfonate (EMS) generated mutant *apa1331* and CRISPR/Cas9 mediated knock-out lines displayed a significant reduction in seed setting rate due to loss of function of *OsSUBSrP1*. Thus, we propose that a mutation in *OsSUBSrP1* produces defects in anther cuticle biosynthesis and triggers ROS accumulation. Our data present the first insight into the novel role of *OsSUBSrP1* in seed setting rate by regulating wax and cutin pathway.

Materials and methods

Experimental materials

The panicle mutant *apa1331* was derived from an *indica* maintainer line Yixiang 1B (WT) by EMS mutagenesis. *Apa1331* was screened from an M_2 population, and the trait of apical abortion was stably inherited. Yixiang 1B is a backbone maintainer line of *indica* hybrid rice, bred from the Institute of Agricultural Sciences, Yibin, Sichuan, China. More than 50 hybrids have been released using its corresponding CMS Yixiang 1A as the maternal parent. The *apa1331* was used as a female parent and crossed with the WT and 02428 (*japonica*) cultivars to construct two F_2 mapping populations. Plants were grown under natural conditions in the experimental fields at Rice Research Institute, Sichuan Agricultural University, Chengdu (N30.67, E104.06), or alternatively at Lingshui (N18.47, E110.04), Hainan Province, China.

Scanning electron microscopy

Scanning electron microscopy was performed as described by Chun et al. [53].

DAB staining and quantification of ROS

3,3-Diaminobenzidine (DAB) staining of the spikelets of WT and *apa1331* was done according to a previously described method [54]. ROS was quantitatively measured in the form of H_2O_2 from 6 cm fresh panicles of WT and *apa1331* using a ROS assay Kit (Beyotime, Shanghai, China) by following a method of Zafar et al. [5].

Trypan blue staining and quantification of malondialdehyde (MDA) contents

Trypan blue staining of WT and *apa1331* spikelets was performed according to Zafar et al. [55]. MDA contents were quantified from 6 cm fresh panicles of WT and *apa1331* using an MDA assay kit purchased from Nanjing Jiancheng Bioengineering Institute according to the manufacturers instruction.

Transverse sectioning of anthers

Different stages of anther development were selected from WT and *apa1331* panicles as previously described by Wilson et al. [56]. Paraffin-embedded anthers were cut into 4 thin slides using a microtome (LEICA RM2255).

TUNEL assay

The samples were selected at the 13 cm stage of panicle development from WT and *apa1331* prepared according to protocol mentioned in the study of Zafar et al. [5].

Quantitative relative expression analysis

RT-qPCR data of genes were determined from the 6 cm panicle tissues taken only from apical spikelets of WT (normal tissues) and *apa1331* (degenerated tissues). PCR amplification and quantitative relative expression were performed according to the previous study of Wu et al. [57].

Genetic analysis of apa1331

Map-based cloning was performed with more than 700 SSR markers using 300 mutant individuals selected from the F_2 population. Polymorphic bands were screened from all the chromosomes. For the MutMap assay, F_2 plants were backcrossed with *apa1331* to generate a BC_1F_2 population. 25 individuals from BC_1F_2 population with apical abortion phenotype were selected, and MutMap analysis was performed according to Abe et al. [58].

Development of knock-out lines using CRISPR/cas9 system

A CRISPR/Cas9 vector (BGK03), carrying rice *U6* promoter and a single-guide RNA (sgRNA), was constructed for targeting *OsSUBSrP1* to develop its knock-out lines. A target sequence (3-CCATGCGCGACCTCAAGTGT-5) with protospacer adjacent motif (PAM) sequence CCA was identified in the first exon of *OsSUBSrP1*. Two oligos were designed using an online Biogle tool (http://biogle.cn/index/excrispr). Knock-out constructs used in the current study were developed using Biogle Biotech Kit (BGK03) purchased from Hongzhou Biogle Biotechnology Co., Ltd. The possible off-target effects were prevented by BLAST search using target sequence in Gramene (www.gramene.org) database. Oligo dimers were synthesized according to the manufacturers guidelines. Briefly, synthesized oligos were dissolved in water to 10 çM. A reaction mixture (18 çl aneal buffer, 1 çl forward oligo and 1 çl reverse oligo) was heated (95 C for 3 min) in PCR, and then slowly reduced to 20 C at a rate of 0.2 C/s. Oligo dimers were constructed into CRISPR/Cas9 vector by mixing the following components (2 çl CRISPR/Cas9 vector, 1 çl oligo dimer, 1 çl enzyme mix and H_2O was added to 10 çl), and kept at a temperature of 20 C for 1 h. The 10 çl of a recombinant mixture containing the CRISPR/Cas9 vector was transformed into an *E. coli* strain Trans-DH5 (100 çl) by following the guidelines of Ma et al. [59]. The mixture was added into preheated liquid LB (700ul) and cultured at 37 C/200 rpm for 1 h. The reaction mixture was plated on the solid LB media having kanamycin at 37 C overnight. Positive clones were confirmed by sequencing from Qingke Biology Co., Ltd. The constructed vector was sent to Boyun Biotechnology Co., Ltd for genetic transformation into the calli of a rice cultivar Zhonghua11 (ZH11) using a method of Toki et al. [60]. The homozygous T_3 plants were used for phenotypic analysis.

Phylogenetic analysis

Sequences of characterized and putative subtilisins were downloaded from NCBI and Phytozome databases and analyzed according to Tripathy et al. [61]. A phylogenetic tree was constructed using a neighbor-joining method at 1000 bootstrap replicate in software MEGA-X [62].

Transcriptome profiling

Transcriptome analysis was performed using three replicates from the panicles of WT and *apa1331*. Total RNA was extracted from 6 cm panicles when the signs of programmed cell death became visible in the apical spikelet of *apa1331* using the manufacturers protocol (mirVana miRNA Isolation Kit, Ambion). A total of 6 samples were sent to OE Biotechnology (Shanghai, China) for complete mRNA transcriptome analysis by following a method reported by Li et al. [63]. Samples integrity was evaluated using the Agilent 2100 Bioanalyzer (Agilent Technologies, Santa Clara, CA, USA). The samples with RNA integrity number (RIN) 7 were subjected to the subsequent analysis. According to the manufacturers instructions, the libraries were constructed using TruSeq Stranded mRNA LT Sample Prep Kit (Illumina, San Diego, CA, USA). Then, these libraries were sequenced on the Illumina sequencing platform (HiSeqTM 2500 or Illumina HiSeq X Ten), and 125 bp/150 bp paired-end reads were generated. The

functional annotation of DEGs was performed according to significantly enriched biological processes according to a GO Consortium [64].

Analysis of anther wax and cutin

The fatty acids contents were determined using 25 mg of fresh anthers from WT and *apa1331* according to the instructions of Jung et al. [35] through GCMS (Gas Chromatograph-2010 Plus SHIMADZU). Briefly, the weighed anthers samples were crushed into powder with liquid nitrogen. A lipid extraction buffer containing chloroform, methanol and water (8:4:3 vol) was added to the sample and vortexed for 1 min. The reaction mixture was sonicated in ice for 5 min, and the process was repeated 35 times and kept standing for 2 h. The mixture was centrifuged at 3000 rpm for 15 min. The chloroform residue was transferred into a 10 ml tube. The residue was washed twice by adding 3 ml of extraction buffer, and obtained chloroform was transferred to the previously mentioned 10 ml tube. The tube was placed in a vacuum drier to extract plant triglycerides. For saponification, 2 ml of a solution (KOH-CH$_3$OH, 0.5 mol/L) was added to the reaction tube, sealed and vortexed for 1 min. The reaction tube was placed in boiling water until the oil droplet completely disappeared from the surface. The reaction was mixed several times during saponification to get all free fatty acids. For methyl esterification, the reaction mixture was cooled for 3 min, and 2 ml of BF$_3$-CH$_3$OH was added, vortexed (10 s) and placed in a water bath (80$^-$C). For extraction, 1 ml of n-hexane and 5 ml of saturated NaCl solution were added to the mixture, vortexed and centrifuged at 2000 rpm for 5 min. The n-hexane layer (not less than 500 çl) was inserted into the Gas Chromatograph. The composition of fatty acids was presented in the form of relative percentage as performed by Liu et al. [65]

Results

apa1331 displayed aborted apical spikelets

To understand the genetic regulation of panicle development, we identified a mutant named *apical panicle abortion1331 (apa1331)*, which shows a stable phenotype of panicle abortion. This mutant was screened through an EMS mutagenized population of a maintainer line (Yixiang 1B), taken as WT in the current study.

At maturity, *apa1331* showed abortion of apical spikelets and had significantly lower seed yield than WT (Fig. 1, A). The panicle of *apa1331* started to develop aborted spikelets at apical portions, while WT did not reveal any abortion (Fig. 1, B). To differentiate, when *apa1331* started to show abortion, we carefully observed different stages of panicle development and compared them with WT (Fig. 1C). Until the 5 cm length of the panicle development, the developmental course of *apa1331* was normal like that of WT and did not reveal any visible abortion signs. At 6 cm length of panicle development, spikelet abortion became visible in the apical spikelets of *apa1331*. Apical spikelets began to degenerate when panicle was still enclosed in the flag leaf. As the panicle grows in its length, apical spikelets abortion became severe. The 6 cm length of panicle development was regarded as the stage of divergence between *apa1331* and WT. Various agronomic traits, e.g., plant height, number of primary branches, number of tillers, and 1000-grain weight did not show any significant differences in *apa1331* compared to WT (Fig. 1D-F). However, the number of grains per spike and fertile panicle length were significantly decreased in *apa1331* (Fig. 1G-H). Degeneration rate, which is the percentage of degenerated/aborted spikelets to the total number of spikelets in a panicle, in *apa1331* was up to 53% (Fig. 1I). At the same time,

WT did not show abortion of spikelets. The seed setting rate in *apa1331* was decreased up to 4053% compared to WT. Thus, *apa1331* is an apical panicle abortion mutant and significantly reduces the number of fertile spikelets and causes a massive loss in grain yield.

The apical spikelets of apa1331 are pollen-less and defective in anther cuticle formation

To know the basis of the low seed setting rate of *apa1331*, we studied the detailed structure of the apical spikelet using stereo and electron microscopy. The anthers of *apa1331* were degenerated, while WT anthers were normal and yellowish (Fig. 2A-B). WT anthers had normal and viable pollens that were darkly stained in potassium iodide (KI) staining, while *apa1331* anthers were entirely pollen-less (Fig. 2C-D). It is worth mentioning that the basal spikelets of *apa1331* were normal and showed fertile spikelets comparable to WT. However, the only apical spikelets were found sterile. Previous studies have revealed the defective development of anthers cuticle in sterile mutants [29,66]. Accordingly, the scanning electron microscopic (SEM) observation revealed a presence of three-dimensional nano-ridges of cuticle on the surface of WT anthers, while *apa1331* showed a complete lack of cuticle (Fig. 2E-H). The lack of cuticle formation on the surface of *apa1331* anthers encouraged a further deep look into microsporogenesis and meristem development. SEM of *apa1331* did not show any observable aberration in meristem formation at 1.5 cm length of panicle (Fig. 2I-J). This data suggests that *apa1331* showed defective anther cuticle formation and did not show any abnormality at meristem development.

Post-meiotic microspore development was defective in apa1331

To reveal any cytological defects in microspore development, cross-sections of different stages of anthers were analyzed as discussed by Wilson et al. [56]. Transverse sections of WT and *apa1331* anthers did not reveal any observable difference until stage 7, and both showed a regular structure of all layers e.g., epidermis, endothecium, middle layer and tapetum (Fig. 3A-D). During the early stage 8, the PMCs of WT went under normal meiosis; however, the PMCs nuclei of *apa1331* were neither round (asterisk) nor enclosed by a well-developed callose wall (Fig. 3E-F). Moreover, the cytoplasm of *apa1331* was trapped within a cloud (Fig. 3F). During late stage 8, in *apa1331,* the cloud around the cytoplasm became more evident, and PMC nuclei were irregular (asterisk) and degenerative (Fig. 3G-H). In contrast, PMC nuclei of WT were darkly stained and showed a regular (round) shape (Fig. 3G). During stage 9, WT tapetum cells were normal, but that of *apa1331* were swollen and significantly degenerated microspore cells and nucleus were seen (Fig. 3I-J). Microspore development of *apa1331* was seriously affected after stage 9 and showed severe degeneration of microspores (Fig. 3K-L). During stage 10, the tapetum of WT started to degenerate, and microsporocytes were found vacuolated. However, the microspores of *apa1331* were collapsed and remnants of degenerated microspores were present in the form of cellular debris (Fig. 3L). Due to severe degeneration in *apa1331* anthers, we were unable to differentiate later stages of development. The results of cross-sections morphology suggest that microspore development after meiosis was strongly affected in *apa1331*.

Reduction of wax and cutin contents in apa1331 anthers

SEM of anthers surface revealed a pronounced lack of cuticle in *apa1331*. To confirm the differences of wax and cutin, which are important components of anthers cuticle, we measured the fatty
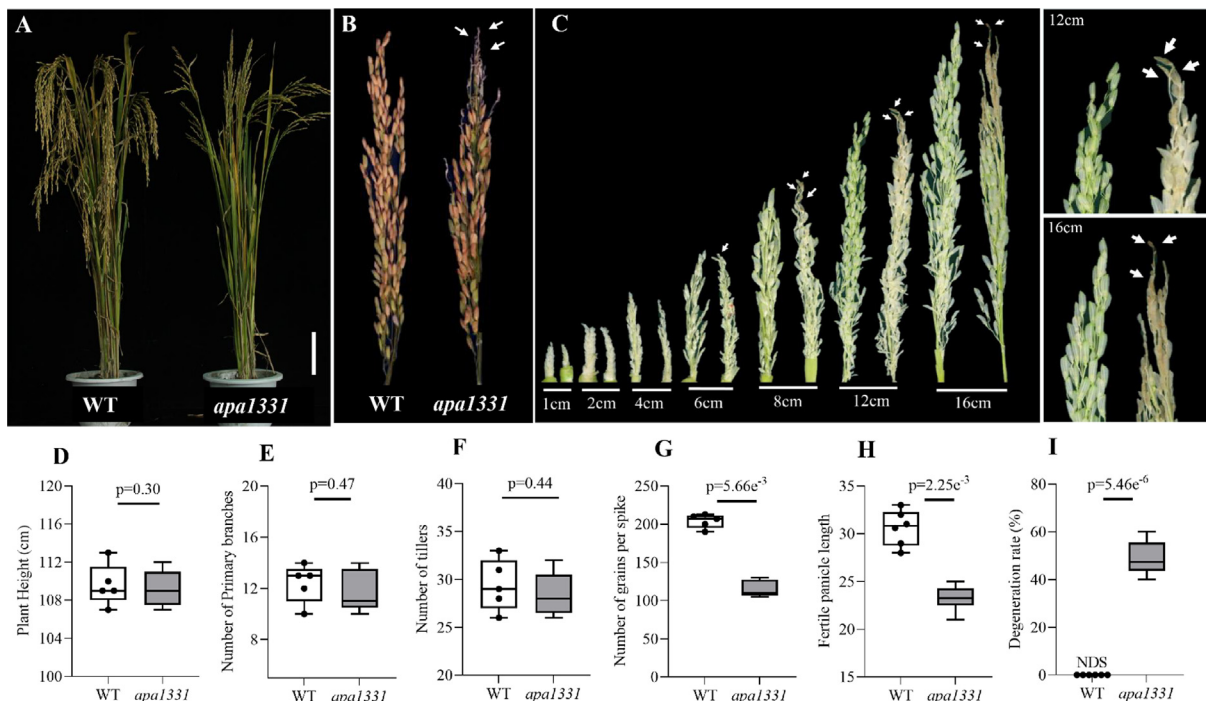
Fig. 1. Phenotypic observation and agronomic traits of *apical panicle abortion1331 (apa1331)*, **(A)** Plant morphology of a Wild Type (WT) plant showing normal panicle development, while an *apa1331* plant shows apical spikelet abortion grown under field conditions. **(B)** Mature panicle of WT and *apa1331*. **(C)** Different stages of WT and *apa1331* panicle at a length of 1 cm, 2 cm, 4 cm, 6 cm, 8 cm, 12 cm and 16 cm. White arrows show the aborted spikelets in *apa1331*. Panels to the right of **C** are enlarged views of 12 cm and 16 cm panicles of WT and *apa1331*. Box and whisker plots **(D-I)** show the comparison of plant height **(D)**, number of primary branches **(E)**, number of tillers **(F)**, number of grains per spike **(G)**, fertile panicle length **(H)** and degeneration rate between WT and *apa1331* **(I)**, respectively. The students *t*-test was used to calculate the significance of the data. Whereas, NDS: no degenerated spikelets. Bars are equal to 10 cm in **(A)**.
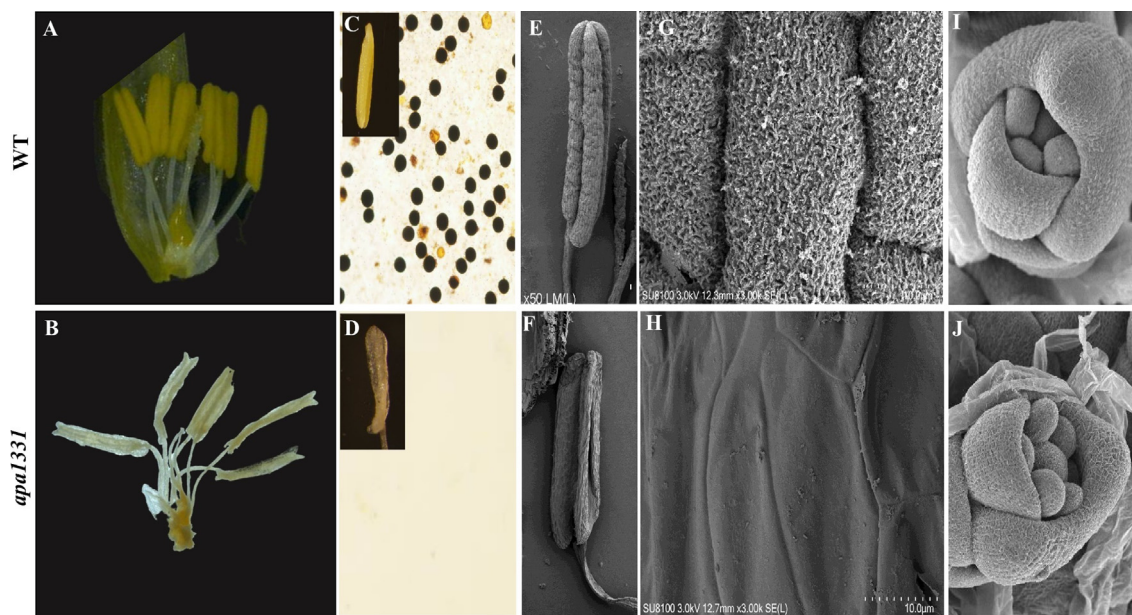
Fig. 2. Microscopic examination and anther cuticle formation of Wild type (WT) and *apical panicle abortion1331 (apa1331)*. **(A-B)** Comparative morphology of WT and *apa1331* spikelet obtained by stereomicroscope. **(C-D)** Potassium iodide (KI) staining of pollens and their enlarged view of WT **(C)** and *apa1331* **(D)**. **(E-F)** Scanning electron micrographs (SEM) of anthers of WT **(E)** and *apa1331* **(F)**. **(G-H)** Zoomed view of anther cuticle surface of WT **(G)** and *apa1331* **(H)**. **(I-J)** Inflorescence meristem development of WT **(I)** and *apa1331* **(J)**. Bars are equal to 1.5 mm in **A-B**, 0.5 mm in **C-D**, 50 çm in **G-H** and 500 çm in **I-J**.

acid profiles of *apa1331* and WT anthers by Gas Chromatography. Composition data of wax and cutin were presented in percentages as described by Liu et al. [65]. Results revealed a significant (P < 0.01) decrease in total cutin and wax contents in *apa1331* as compared to WT (Fig. 4A-B). Among saturated fatty acids, palmitic

acid (C16:0) and steric acid (C18:0) constitute the cutin monomers and were significantly (P < 0.01) decreased in *apa1331* as compared to WT (Fig. 4C). Similarly, the percentage of saturated wax, especially C15:0, C17:0 and C20:0 were also significantly reduced in *apa1331* (Fig. 4D). Similarly, unsaturated cutin e.g., C16:1,
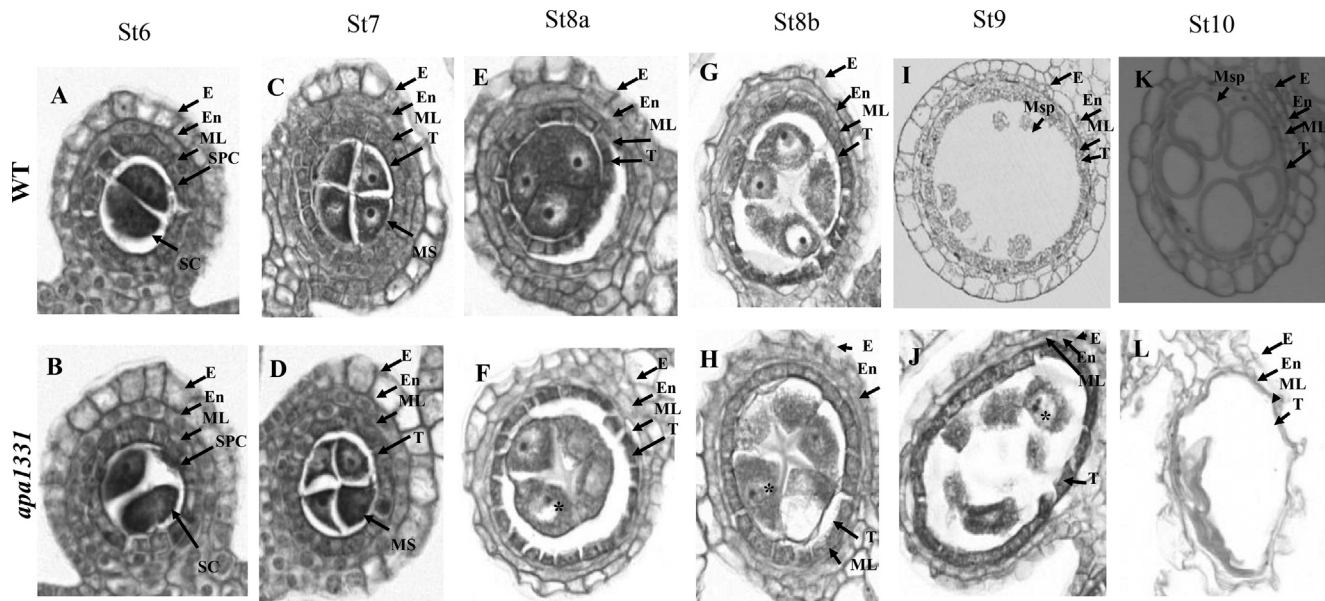
Fig. 3. Transverse sections of anthers showing defects of microspore development in *apical panicle abortion1331 (apa1331)*. (A-L) Transverse micrographs of Wild type (WT) and *apa1331* anthers development at (A-B) St6: showing normal thickening of anthers walls, (C-D) St7: showing the normal development of all anther layers in *apa1331*, (E-F) St8a: showing the trapped cytoplasm in a cloud, and degeneration of pollen mother cell (PMC) nucleus in *apa1331*. At the same time, the PMC of WT was regular and round. Asterisk (*) indicates the position of degenerating PMC nucleus. (G-H) St8b: Trapped cytoplasm and degeneration of PMC nucleus of *apa1331* become more evident, (I-J) St9: Swollen tapetum and degeneration of microspore of *apa1331*, (K-L) St10: At late microspore mother cell development, *apa1331* showed complete degeneration of microsprocyte in the form of a degenerated tissue. Whereas, **E**; epidermis, **En**; endothecium, **ML**: middle layer, **SPC**; secondary parietal cells. **SC**; sporocytes, **T**; tapetum, and **Msp**; microsporocyte. Bars in **A-L** are 25 μm.
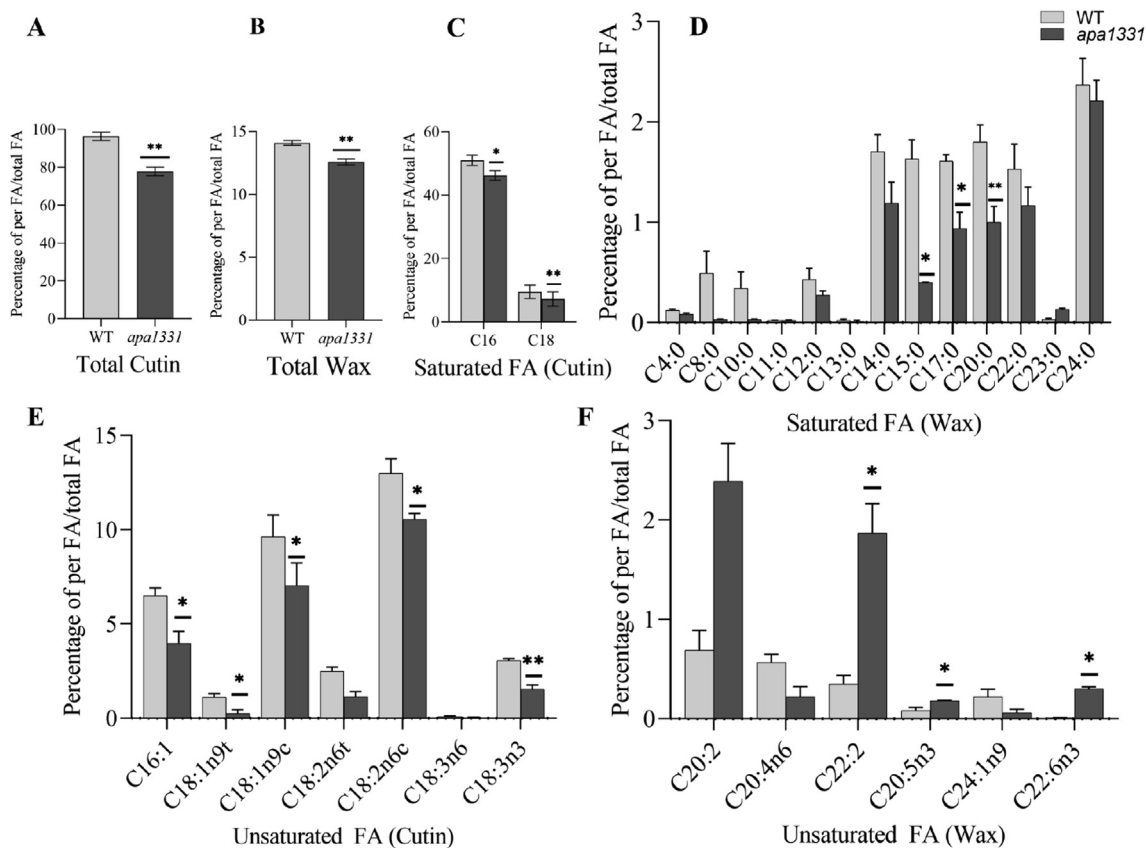
Fig. 4. Composition of wax and cutin contents in anthers of Wild type (WT) and *apical panicle abortion1331 (apa1331)*, (A) Total amount of cutin in anthers. (B) Total amount of wax in anthers. (C) Amount of saturated fatty acids (cutin) in anthers. (D) Amount of saturated fatty acids (wax) in anthers. E) Amount of unsaturated fatty acids (cutin) in anthers. (F) Amount of unsaturated fatty acids (wax) in anthers of WT and *apa1331*. The values represent the average of three individual repeats. Data in (A-F) are presented in percentages of per fatty acid to total fatty acids. The students *t*-test was used to calculate the significance of data, where *$p < 0.05$ and **$p < 0.01$.
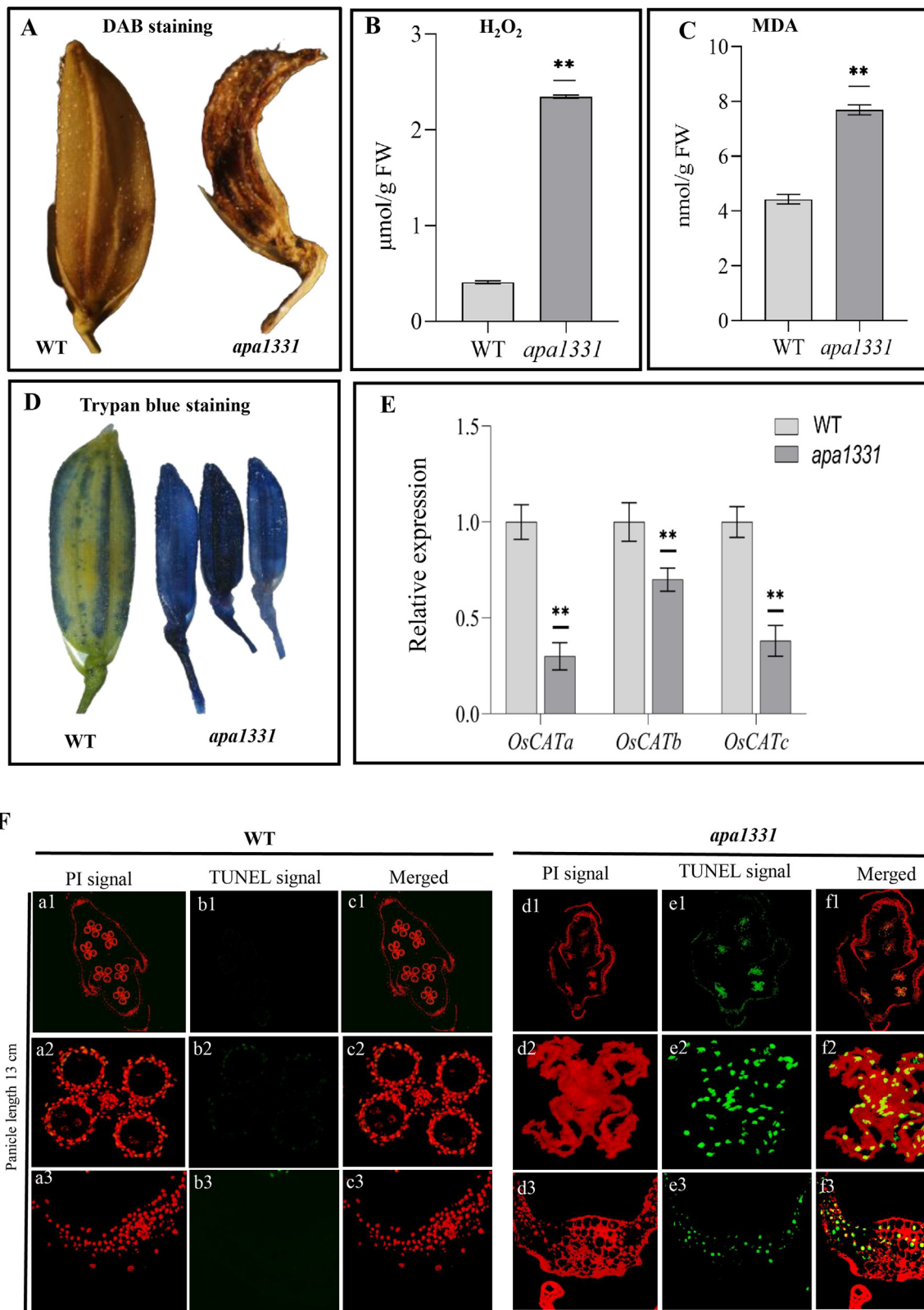
Fig. 5. Analysis of reactive oxygen species (ROS), cell viability, cell death and DNA fragmentation in *apical panicle abortion1331 (apa1331)*, (A) Dark DAB (3,3–diaminobenzidine) staining of the spikelet of *apa1331* shows the excessive accumulation of hydrogen peroxide (H_2O_2) compared to WT. **(B)** Quantification of H_2O_2 was significantly increased compared to WT. **(C)** Quantification of malondialdehyde (MDA) was significantly increased compared to WT. **(D)** Trypan blue staining revealed the compromised cell viability in apical spikelet *apa1331*. **(E)** Significant downregulation of *CATALASES*, e.g., *OsCATa*, *OsCATb* and *OsCATc* in the panicle of *apa1331* than WT. **(F)** TUNEL (terminal deoxynucleotidyl transferase dUTP nick end labeling) assay showing DNA fragmentation in spikelet of *apa1331*. Tissues were taken from the whole spikelet (**a1** and **d1**), anther (**a2** and **d2**) and glume (**a3** and **b3**). Propidium iodide (PI) and *iso*-thiocyanate produce red and green (**b** and **e**) fluorescence, respectively. Yellow (**c** and **f**) fluorescence is the combined signals of PI and *iso*-thiocyanate. (For interpretation of the references to color in this figure legend, the reader is referred to the web version of this article.)

C18:1nt, C18:1nc and C18:1n3 were also significantly decreased in *apa1331* (Fig. 4E). However, contrary to other fatty acids, unsaturated wax contents e.g., C22:2, C20:5n3, and C22:6n3 were significantly (P < 0.05) increased in *apa1331* compared to WT (Fig. 4F). Consistent with our previous observations, chemical composition analysis of wax and cutin revealed that the candidate gene of *apa1331* regulates the wax and cutin contents and anther cuticle formation.

Apical spikelets of apa1331 had higher level of ROS

Excessive ROS accumulation could happen either due to genetic factors or in response to biotic and abiotic stresses [67]. These ROS molecules could cause damage to the cell wall structure, macromolecules, DNA and proteins, leading to the degenerated tissues [68]. To further investigate the cause of abortion of spikelets of *apa1331,* we detected the cellular ROS by DAB staining (Fig. 5A).

The quantitative measurements revealed that H_2O_2 was significantly (P < 0.01) increased in apical spikelets of *apa1331* than that of WT (Fig. 5B). Malondialdehyde (MDA) is an indicator of local ROS production and is involved in the peroxidation of fatty acids [69]. Consistently, MDA was also significantly increased in *apa1331* spikelets (Fig. 5C). Trypan blue staining is used to test the viability of cells [70]. Dark staining of the apical spikelet of *apa1331* showed cells viability was compromised, while light staining of WT showed spikelets cells were viable (Fig. 5D). *CATALASE (OsCATa), OsCATb,* and *OsCATc* are antioxidant enzymes coding genes and are involved in the scavenging activities of ROS [71]. Relative expressions of *OsCATa, OsCATb,* and *OsCATc* were significantly decreased in *apa1331* spikelets compared to WT (Fig. 5E, Table S1). Together, DAB staining, measurement of H_2O_2 and relative expression data revealed the excessive accumulation of ROS in *apa1331* caused the abortion and damage to apical spikelets. At the same time, trypan blue staining has indicated the death of apical spikelets cells.
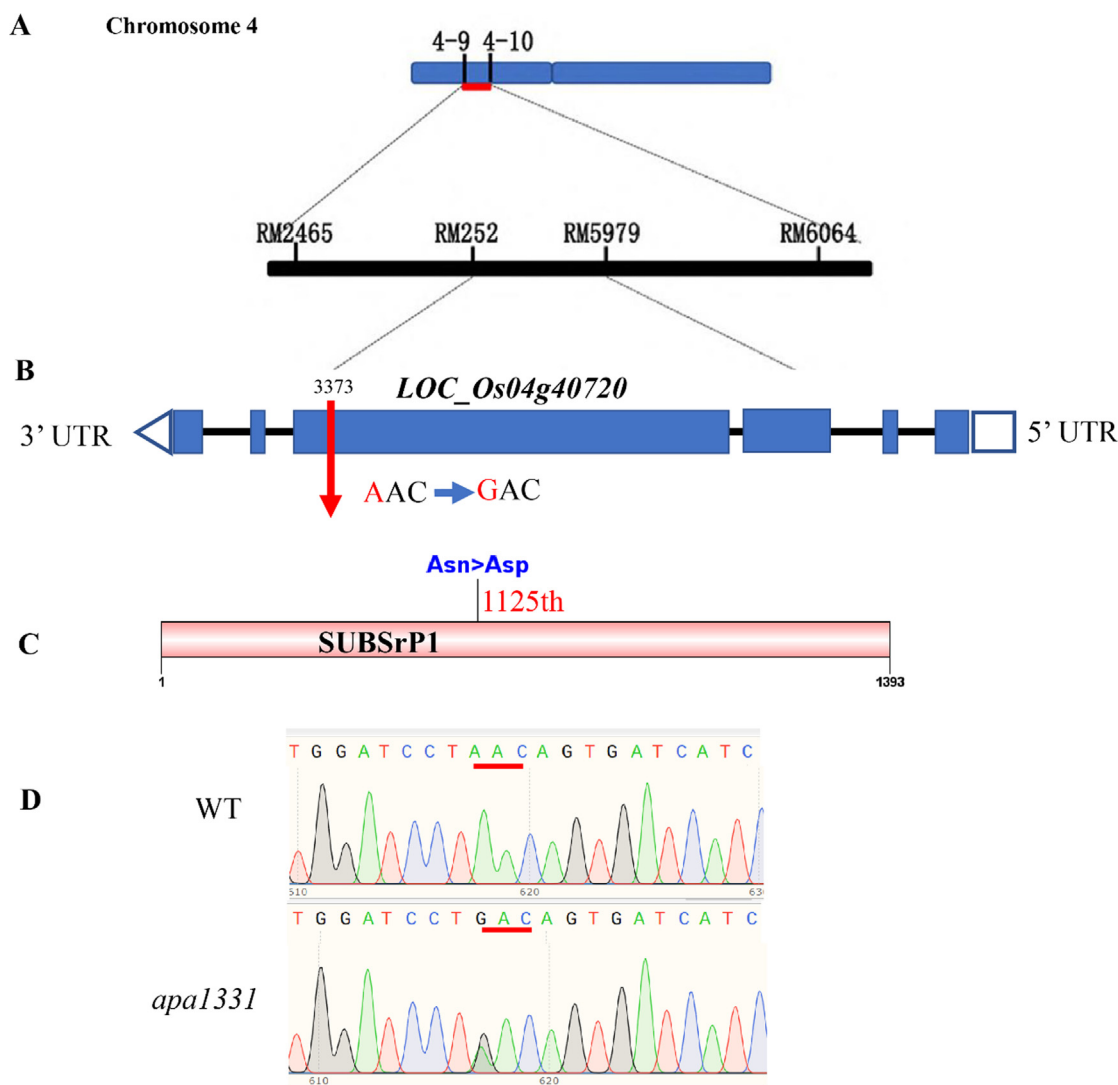
Fig. 6. Fine mapping and genetic analysis of *SUBTILISIN-LIKE SERINE PROTEASE 1 (OsSUBSrP1)*. (A) Primary mapping of the *OsSUBSrP1* controlling *apical panicle abortion1331 (apa1331)* phenotype on chromosome 4 between SSR markers 49 and 410. (B) Genomic structure of *OsSUBSrP1 (LOC_Os04g40720)* and position of an SNP, where blue boxes are representing exons, blue lined boxes are up and downstream sequences and black lines are indicating introns. The red arrow shows the position of an SNP that was harbored in the 4th exon of *OsSUBSrP1.* (C) SUBSrP1 was consist of 1393 amino acids, and black line show the position of a non-synonymous substitution (Asn > Asp) of 605th amino acid. (D) The comparative chromatograms cloned and sequenced from WT (up) and *apa1331* (down), where the red lines show the substituted sequence (AAC > GAC) of the codon. (For interpretation of the references to color in this figure legend, the reader is referred to the web version of this article.)

Apical spikelets and anthers of apa1331 showed increased cell death and DNA fragmentation

Trypan blue staining indicated the presence of cell death in apical spikelets of *apa1331*. We hypothesized that apical spikelets of *apa1331* would have undergone an abnormal PCD and DNA fragmentation. To test this hypothesis, we performed a TUNEL (terminal deoxynucleotidyl transferase-mediated dUTP nick-end labeling) assay to detect apoptosis. Spikelet and anthers of 13 cm panicle length were used as representatives (Fig. 5F). WT (Fig. 5-Fa-c) showed the absence of TUNEL signal in all parts of spikelets (c1) including anther (c2) and glume (c3). However, *apa1331* (Fig. 5Fd-f) showed positive TUNEL signals in all parts of the spikelet (e1) including anther (e2) and glume (e3). These findings suggest that DNA fragmentation has occurred in *apa1331* at the single-cell level that causes cell death in spikelets and anthers.

OsSUBSrP1 encodes a putative protein of a subtilisin family

To find the candidate gene of the characterized mutant phenotype, we developed two F₂ mapping populations. These mapping populations were derived by crossing *apa1331* with an *indica* cv. Yixiang 1B and a *japonica* cv. 02428, respectively. In F₁ generations of both populations, all plants did not show an abortion phenotype. Genetic analysis of these populations revealed that a single reces-sive gene controls the phenotype of panicle abortion in *apa1331* [52].

Primary mapping of *apa1331* revealed that the candidate gene resides between the SSR marker 49 and 410 on the short arm of chromosome 4 (Fig. 6A). The gene was narrowed down between RM252 and RM5979 in a distance of 16.4 cM [52]. Due to the further unavailability of InDel markers in this region, we performed a MutMap assay to find any mutation in the primary mapped region by following a method of Abe et al. [58]. MutMap whole genome sequencing (Illumina HiSeq 2500 platform) revealed an SNP index of 1 due to the presence of a single nucleotide mutation in (*Os04g0483400*) *LOC_Os04g40720* [52]. Consistent with the primary mapping by SSR markers, Mutmap results showed an SNP (A > G) located between the previously mapped region of SSR markers RM252 and RM5979. According to MutMap, the candidate gene of *apa1331* phenotype was *LOC_Os04g40720*, and it has six exons, present in reverse order in the MSU database. The mutation was located in the 4th exon of *LOC_Os04g40720*, changing the 3373th codon from AAC to GAC (Fig. 6B). This SNP in *apa1331* has ultimately substituted an amino acid (asparagine into aspartic acid). According to Rice Genome Annotation Project (http://rice.plantbiology.msu.edu/), *LOC_Os04g40720* annotates a putative protein of *SUBTILISIN LIKE SERINE PROTEASE* [72]. Candidate protein has a total residue length of 1393 amino acids, and mutation (Asn > Asp) was occurred in 1125th amino acid (Fig. 6C). To further verify the
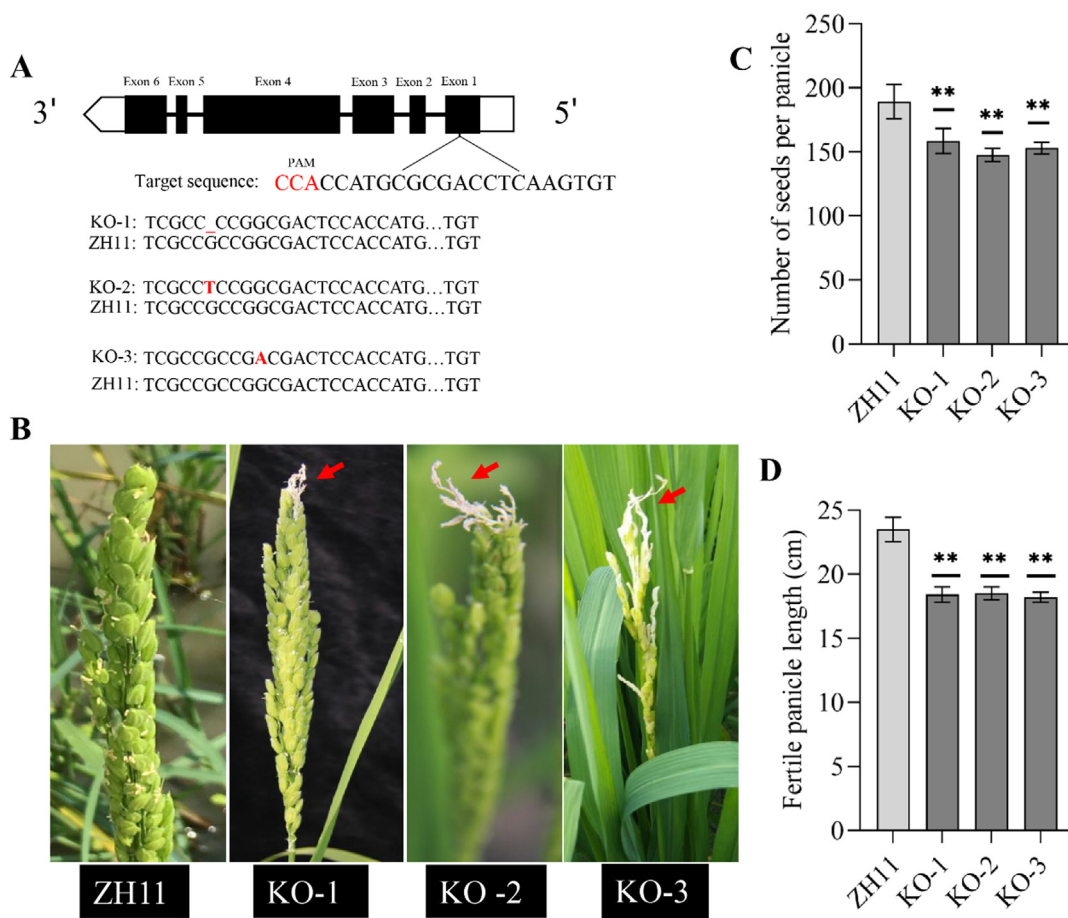
Fig. 7. CRISPR/Cas9 mediated knock-out (KO) lines of *SUBTILISIN-LIKE SERINE PROTEASE 1 (OsSUBSrP1)* showed the phenotype of apical abortion. (A) The position of target sequence (PAM and gRNA) in gene structure of *OsSUBSrP1*. Sequence comparison reveals a one bp (-) deletion in KO-1, substitution of G to T in KO-2 and substitution of G to A in KO-3 **(B)** Panicle of KO-1, KO-2, and KO-3 show the phenotype of apical abortion, while the Zhonghua11 (ZH11) did not show abortion. **(C)** Number of seeds per panicle was significantly (P < 0.01) decreased in KO-1, KO-2, and KO-3. **(D)** Fertile length of panicle was significantly decreased due to apical panicle abortion in KO-1, KO-2, and KO-3. The students *t*-test was used to calculate the significance of data, whereas **p < 0.01.
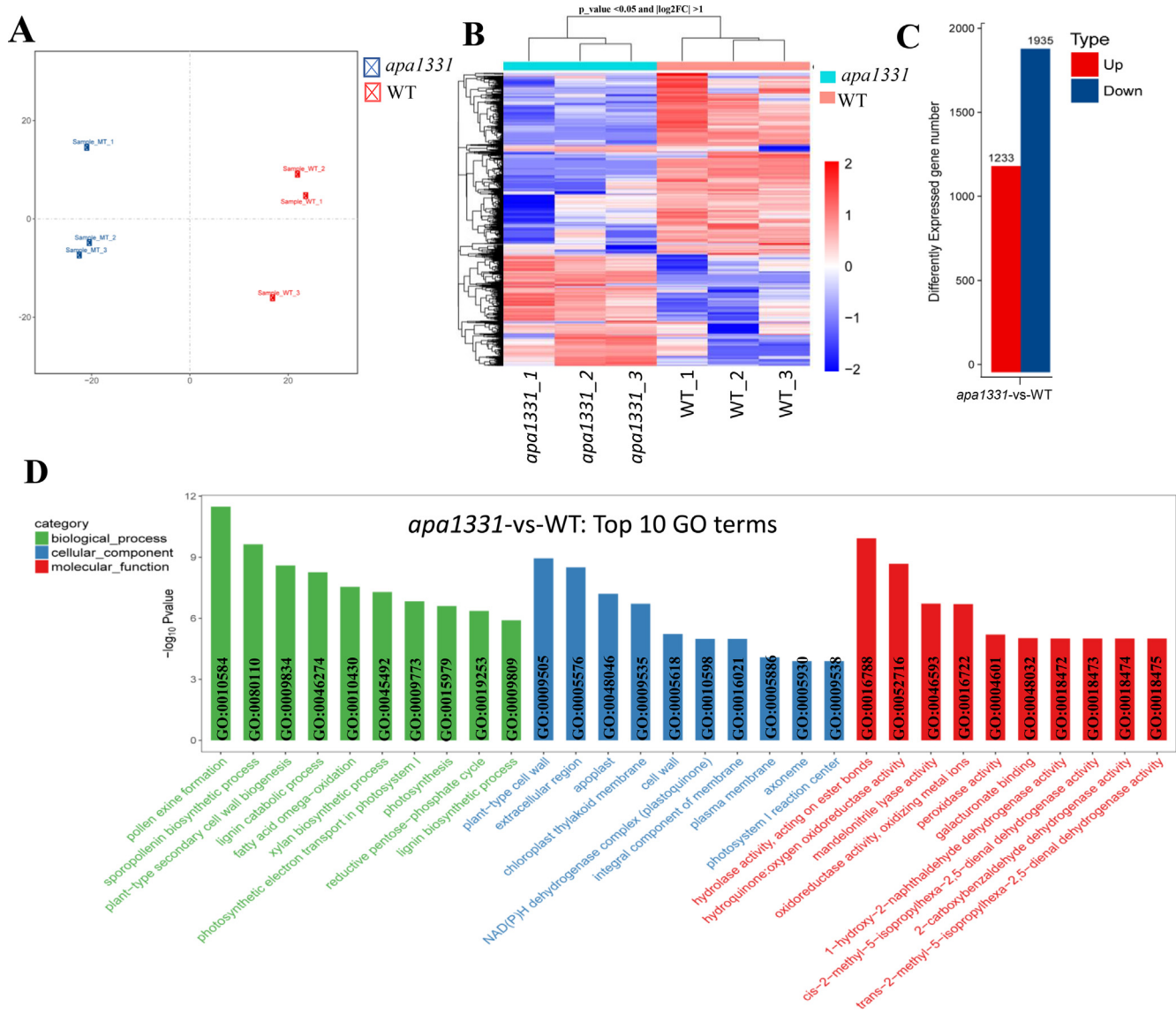
Fig. 8. **Global gene expression analysis of Wild type and** *apical panicle abortion1331,* **(A)** Principal component analysis (PCA) shows 76% and 19% variations in the samples contributed by PC1 and PC2, respectively. **(B)** Heat map showing the differentially expressed genes (DEGs) with log2FC > 1 at *p*-value < 0.05 in *apa1331* compared to WT. **(C)** Graph showing statistics of DEGs between WT and *apa1331,* where red and blue color are showing the number of up and down-regulated genes, respectively. **(D)** Comparison of top 30 downregulated gene ontology (GO) terms. The x-axis shows the GO terms of biological processes, cellular components and molecular functions in green, blue and red color, respectively, while the y-axis shows the -log$_{10}$ (*p*-value) of differentially enriched GO terms between WT and *apa1331.* (For interpretation of the references to color in this figure legend, the reader is referred to the web version of this article.)

MutMap candidate gene analysis, we cloned and sequenced the candidate gene *LOC_Os04g40720* in *apa1331* and WT. The comparative chromatograms of WT and *apa1331* validated the presence of an SNP at the same position consistent with MutMap analysis (Fig. 6D).

Phylogenetic and annotation analysis of the candidate gene of *apa1331* shows that it encodes a novel protein and has not been characterized before. However, its orthologs in Brachypodium (Bradi5g13740), maize (GRMZM2G063163) and sorghum (Sb06g0200570) encode putative subtilisin-like serine proteases. According to MEROPS database, there are more than 50 families of serine protease [73]. A study has identified 63 and 56 subtilases in rice and *Arabidopsis*, respectively [74,75]. These two plant species also appear to encode a similar number (206 and 222) of putative subtilises in *Arabidopsis* and rice, respectively [61]. Although the

genome size of rice (389 MB) is much higher than that of *Arabidopsis* (125 MB). Another genomic evolution study has categorized serine protease into 9 families, among them subtilisins are the second largest family having a catalytic triad of Asp (D), His (H) and Ser (S) residues with no other structural similarity [76,77]. Accordingly, the candidate protein of *apa1331* has also no known structural similarity with other characterized proteins. BLAST of referenced protein showed only a 37–45% sequence similarity with most of the uncharacterized proteins of species other than rice (Figure S1). None of the members of its orthologs genes have been functionally characterized before. Amino acid sequence alignment of blasted proteins showed conserved residues of catalytic triads of D, H and S (Figure S2 A). A phylogenetic tree was constructed, revealing rice subtilisins can be divided into three major clades (Figure S2 B). The largest clade shared 26 genes that were further divided into

two subclades. While both second and third clades shared two genes each. The reference gene (Os04g0483400) was placed into a seprate clade with another gene Os07g0651400.

Genetic analysis revealed that a-synonymous subtitution (Asn-Asp) of an amino acid in *apa1331* has not occurred in the catalytic triad of subtilisin. It suggests the additional and criticle role of another amino acid (Asn) combined with other catalytic traids for proper functioning. The presence of a catalytic triad of D, H and S and functional homology with subtilisin orthologs suggest that the candidate protein of *apa1331* encodes a subtilisin. Hence, we tentatively named the reference protein of *apa1331* as putative SUBSrP1.

SUBSrP1 is preferentially expressed in the upper part of a young panicle

Members of the subtilisin protease family showed variation in spatio-temporal expression under different conditions [78]. According to Rice anther expression (https://www.cpib.ac.uk/an-ther/riceindex.html) plots [79] the expression of *OsSUBSrP1* during anther development was also found variable (Figure S3 A). According to BAR ePlant Browser [80] database (bar.utoronto.ca/eplant) relative expression spectrum of *OsSUBSrP1* showed the highest expression in a young panicle at stage P1 and P2 (Figure S3 B). To answer an important question, e.g., why only apical spikelets of *apa1331* have degenerated? We determined the relative expression spectrum of *OsSUBSrP1* in the root, leaf, stem and different stages of panicle development in WT (Figure S4). Relative expression of *OsSUBSrP1* in 5 cm panicle was higher than that of 2 cm and 12 cm panicle length. We further divided the 5 cm panicle into the upper, middle and lower part and quantified the relative expression of *OsSUBSrP1*. Result revealed that *OsSUBSrP1* was preferentially expressed in different parts, where upper part showed highest expression followed by middle part, and minimum in lower part of WT panicle. Variation in the expression of *OsSUBSrP1* redundancy between different parts of the panicle disentangled its

phenotypic defect from the lower and middle part of the panicle. Hence, the phenotypic defect of the loss of function of *OsSUBSrP1* was majorly seen in the apical spikelets only.

CRISPR-Cas9 targeted knock-out lines showed the phenotype of apical spikelet abortion

To validate the function of *OsSUBSrP1*, a CRISPR-*Cas9* vector containing a sgRNA was constructed and transformed into calli of ZH11 to develop knock-out (KO) lines. The target sequene sequence (3- CCATGCGCGACCTCAAGTGT-5) was located in first exon of *OsSUBSrP1* (Fig. 7A). Three independent knock-out (KO) lines showed the abortion of apical spikelet. Sequencing revealed the one bp (G) deletion, one bp substitution (G to T) and one bp substitution (G to A) in KO-1, KO-2, and KO-3, respectively. KO-1, KO-2 and KO-3 showed the abortion of apical spikelets, while the ZH11 did not show any abortion phenotype at the heading stage (Fig. 7B). Similar to *apa1331*, the number of seeds per panicle and fertile panicle length was significantly (P < 0.01) decreased in KO-1, KO-2, and KO-3 compared to ZH11 (Fig. 7C-D). Overall, genetic analysis of *apa1331* and CRISPR/Cas9-targeted mutagenesis of KO lines revealed that mutation in *OsSUBSrP1* causes a significant decrease in seed setting due to abortion of apical spikelets. It validates the function of *OsSUBSrP1* in apical spikelet development in rice.

Global gene expression analysis revealed OsSUBSrP1 mediated downregulation of wax and cutin biosynthesis pathway genes

Abnormal PCD and elevated ROS levels can affect the expression of many wax and cutin pathway genes [5,39]. To elucidate the transcriptional changes associated with functional pathways due to mutation in *OsSUBSrP1*, a comparative transcriptome profiling of WT and *apa1331* was performed using RNA sequencing Illumina Platform (HiSeqTM 2500). Three individual sampling repeats were selected from WT and *apa1331* apical spikelets at the 6 cm stage
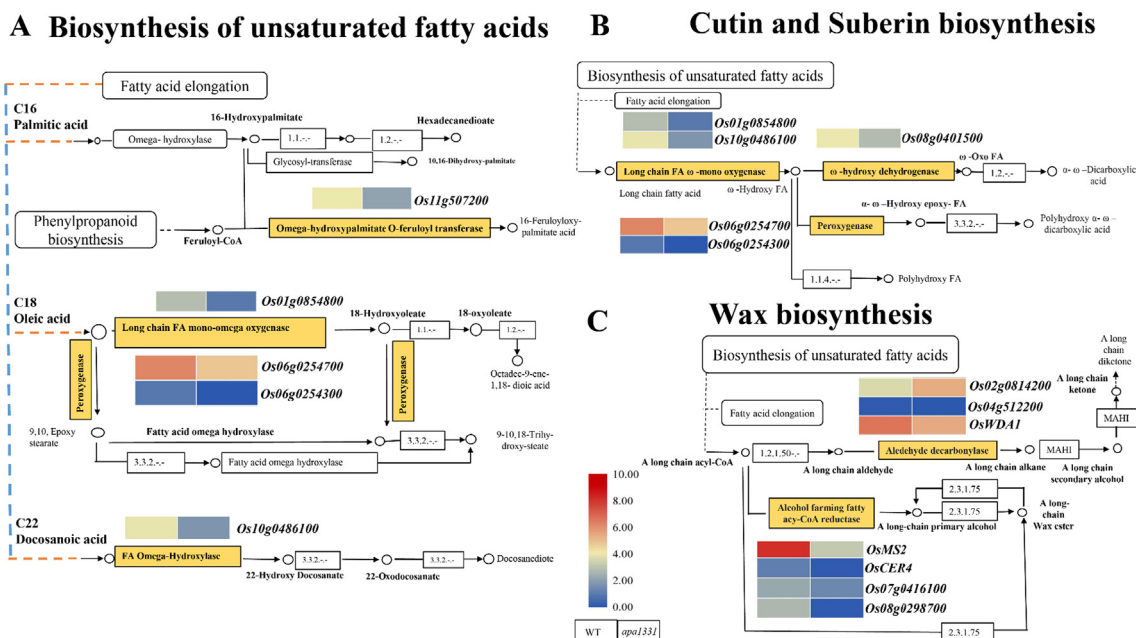
Fig. 9. *SUBTILISIN-LIKE SERINE PROTEASE 1 (OsSUBSrP1)* **regulates the expression of wax, suberin, and cutin biosynthesis pathway genes,** **(A)** Comparative transcriptome analysis of Wild type (WT) and *apical panicle abortion1331 (apa1331)* revealed the downregulation of genes involved in the biosynthesis of the unsaturated fatty acids. **(B)** Comparative transcriptome analysis of WT and *apa1331* revealed the downregulation of genes involved in the biosynthesis of cutin and suberin biosynthesis. **(C)** Comparative transcriptome analysis of WT and *apa1331* revealed the up and downregulation of genes involved in the wax biosynthesis. The heat maps showed the normalized expression value of fragments per kilobase of transcript per million (FPKM) for a specific gene (brown rectangle). Figure legend shows the normalized expression value key scale, in which dark red and blue show the highest and lowest expression, respectively. (For interpretation of the references to color in this figure legend, the reader is referred to the web version of this article.)

(point of divergence between WT and *apa1331*). High-throughput RNA sequencing generated high-quality data with an adequate sequencing depth. Principal component analysis (PCA) revealed 76% (PC1) and 19% (PC2) variance between WT and *apa1331* samples (Fig. 8A). The heat map showed a sum of 3168 differentially expressed genes (DEGs) between *apa1331* and WT (Fig. 8B). Among 3168 DEGs, 1935 and 1233 DEGs were found down-regulated and up-regulated in *apa1331* compared to WT, respectively (Fig. 8C). We further subjected the significantly [fold change (FC) > 2 and a *p* < 0.05] DEGs to gene ontology (GO) enrichment analysis and Kyoto encyclopedia of genes and genomes (KEGG) pathway functional classification.

GO enrichment analysis of significantly enriched DEGs between *apa1331* and WT was categorized into biological processes, cellular components and molecular functions. Among the top 30 down-regulated DEGs, pollen exine function (GO:0010584) was most significantly down-regulated biological process in *apa1331* (Fig. 8D). While other important biological processes associated with these downregulated DEGs were sporopollenin biosynthetic process (GO:0080110), fatty acid omega oxidation (GO:0010430) and lignin biosynthetic process (GO:000980). While most significantly downregulated cellular components and molecular functions associated with these DEGs were plant-type cell wall (GO:0009505) and hydrolase activity, acting on ester bonds (GO:00016788), respectively. GO classification indicates the downregulation of pollen exine, sporopollenin, fatty acid omega-oxidation related biological processes in *apa1331* panicle.

We mapped all DEGs to their respective KEGG enrichment analysis to get further insights into the specific pathways, which regulate the above-mentioned biological processes. Among them, the cutin, suberin, and wax biosynthesis pathway (K00073) was the most relevant KEGG pathway with the highest (15.3%) number of DEGs (Fig. 9). 13 DEGs were involved in the wax and cutin biosynthesis pathway. Among the 13 genes, 12 genes *(Os11g0507200, Os01g0854800, Os06g0254700, Os06g0254300, Os10g0486100, Os08g0401500, Os04g0512200, OsWDA1, OsMS2 (MALE STERILITY2), OsCER4, Os07g0416100* and *Os08g0298700)* were significantly down-regulated. While only one gene *Os02g0814200* annotated for aldehyde decarboxylase (EC: 4.1.99.5) was up-regulated (FC = 3.341) in *apa1331* compared to WT. The heat map of these 12 down-regulated and one up-regulated genes represents significant changes in their expression in *apa1331* compared to WT. Among the down-regulated genes e.g., *Os11g0507200* encodes a transferase family protein and is involved in the biosynthesis of unsaturated fatty acids, especially cutin and suberin. *Os01g0854800* and *Os10g0486100* encode a cytochrome P450 protein and are involved in the long-chain fatty acid monooxygenase activity (EC:1.14.14.80). *Os06g0254300* encodes a peroxygenase and is involved in the cutin, suberin and wax biosynthesis pathway. *OsWDA1, OsMS2,* and *OsCER4* have been reported to regulate the wax and cutin biosynthesis and pollen development in rice [30,35,81].

To validate the expression of DEGs obtained in RNA-seq data, we randomly selected five genes among up-regulated and down-regulated DEGs validated their relative expression by RT-qPCR (Figure S5, Table S1). The level of *ENT-COPALYL DIPHOSPHATE SYNTHASE 4* (O*sCPS4*), *CXE CARBOXYLASE, POLYAMINE OXIDASE, DIISOPROPYL-PHOSPHO-FLUORIDATE (DFP)* and *GLUCSOYL HYDRO-LASE* were significantly up-regulated in *apa1331* compared to WT. *LTPL72, PURPLE ACID PRECURSOR, CYTOCHROME P450 FAMILY, 3-OXOACYLE-REDUCTASE* and *OsC6* were significantly down-regulated in *apa1331* compared to WT. The relative expression of genes analyzed by qRT-PCR was consistent with that RNA-seq profiling. These results support that mutation in *OsSUBSrP1* causes a significant decrease in wax and cutin contents due to downregulation of cutin, suberin and wax biosynthesis pathway genes.

Discussion

Successful plant reproduction is a sophisticated process involving proper development of male and female reproductive organs. This process is controlled by a set of different genetic factors working together in different pathways. Identifying the role of these genetic factors is crucial to understand the mechanism of reproduction, and the knowledge could be applied in hybrid-breeding programs to accelerate the crop yields. In this study, we have identified the role of a novel genetic factor called *OsSUBP1* in rice male reproductive development using mutation breeding, transcriptomic and genome editing approaches. The *OsSUBP1* was cloned from a mapping population using map-based cloning based on a panicle abortion mutant called *apa1331*. The function was confirmed by knocking-out the target gene using CRISPR/Cas9, a highly sensitive genome editing approach [82].

OsSUBSrP1 is essential for normal apical spikelet development

Genetic analysis of *apa1331* has revealed that it bears an SNP (A > G) in the 4th exon that causes the dysregulation in *OsSUBSrP1* (Fig. 6). *OsSUBSrP1* encodes a putative subtilisin and its role in the plants was not reported before. A study has indicated the secretion of a serine proteinase at late microsporogenesis and primary expression in tapetal cells [51]. It was also stated that the serine protease is a preprotein, which acquires glycans during movement from the Golgi body and mitochondria to other organelles. Another study revealed the preferential expression of a preprotein *RICE SUBTILISIN-LIKE SERINE PROTEASE 1* (*RSP1*) in ovaries and pistils [50]. Few family members have also been differentially expressed in tomatoes [83]. Martinez et al. reported *SENESCENCE-ASSOCIATED SUBTILISIN LIKE PROTEASE (SASP)* in *Arabidopsis,* and its loss of function mutant showed increased inflorescence branches at the reproductive stage [49]. They also reported that the subtilisin-like SASP function is conserved at-least between rice and *Arabidopsis*. However, functional characterization of any individual plant serine protease has not been reported so far. Nonetheless, some findings have indicated the presence of SUBSrP in rice and preferential expression in flower development [4950]. Our study presents that loss of function of *OsSUBSrP1* produced apical spikelet abortion. Knock-out of *OsSUBSrP1* also produces apical abortion, which verifies its indispensability for normal apical spikelet development in rice.

OsSUBP1 is involved in anther cuticle formation and regulates wax and cutin biosynthesis pathway

Fatty acids are essential molecules required during anther, especially tapetum development [29]. Anthers of the apical spikelets of *apa1331* were pollen-less and sterile. Their SEM also revealed defects in anther cuticle formation (Fig. 2E-G). Transverse sections of *apa1331* revealed the abnormal swelling of tapetum and degeneration of the PMC nucleus at stage 9 (Fig. 3K-L). Anther cuticle is composed of cutin and wax, which are long-chain fatty acids, alcohols and alkanes [84]. Comparative fatty acid profiling revealed a substantial decrease in wax and cutin in *apa1331* (Fig. 4). Previous studies showed that reduction of wax and cutin contents causes defects in pollen development [16,29,42,66]. Decrease in wax and cutin contents also suggests the substantial loss of water and alters cuticle properties [85]. Transcriptome profiling of apical spikelets also revealed the significant downregulation of wax and cutin pathway genes in *apa1331*. Downregulation of wax and cutin genes supports the observation of decreased anther cuticle formation (Fig. 9). Global gene expression analysis revealed that 13 genes were directly involved in the
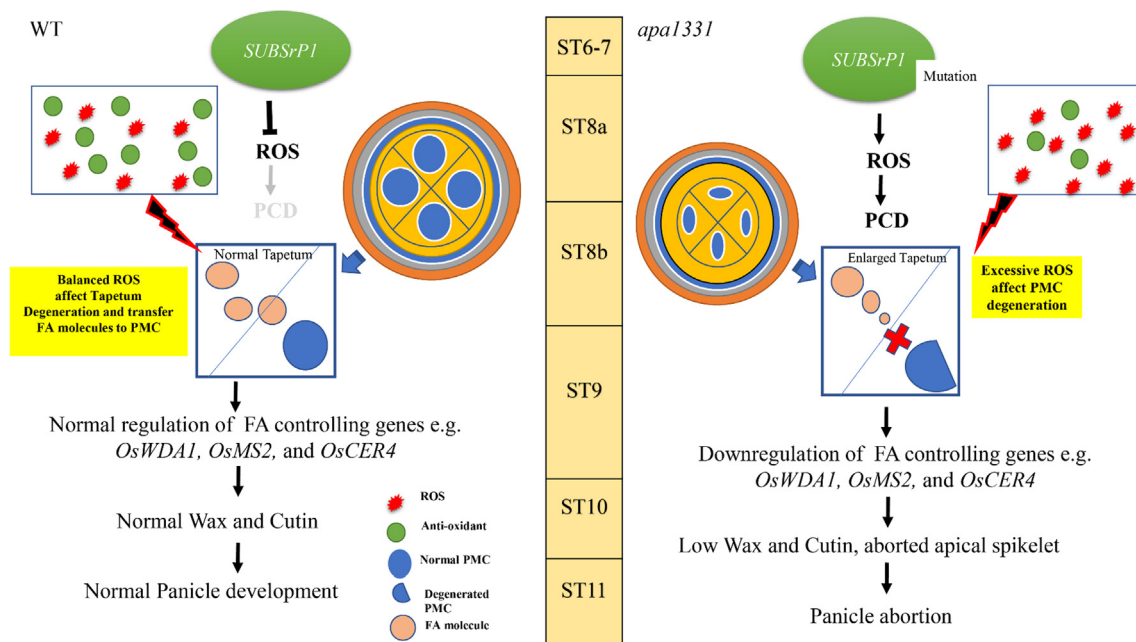
Fig. 10. An Illustration showing the function of *SUBTILISIN-LIKE SERINE PROTEASE 1 (OsSUBSrP1)* in homeostasis of Reactive oxygen species (ROS)-mediated programmed cell death (PCD) for anther cuticle development and seed setting rate, *OsSUBSrP1* is essential for maintaining a balance of ROS-mediated PCD and plays a key role in developing apical spikelets by regulating the expression of wax and cutin pathway genes. A mutation in *OsSUBSrP1* causes dysregulation in its protein and produces a defect in anther cuticle formation in *apical panicle abortion1331* (*apa1331*). Significant decrease of wax and cutin contents in anthers of *apa1331* causes excessive water loss from the surface of anthers that ultimately produce aborted spikelets.

metabolism of fatty acids. *OsWDA1, OsMS2* and *OsCER4* have already been reported to regulate wax biosynthesis, pollen exine and anther walls formation [35,42,65,81]. *Os01g0854800, Os06g0254300* and *Os10g0486100* also encode different enzymes involved in regulating cutin, suberin and wax biosynthesis pathway. A considerable decrease in saturated and unsaturated wax and cutin in *apa1331* was likely due to the down-regulation of genes mentioned above. These findings support that *OsSUBSrP1* is essential for normal development of PMC and anther cuticle formation. Our data suggest *OsSUBSrP1* plays an essential role in anther cuticle formation by regulating the expression of wax and cutin biosynthesis genes.

OsSUBSrP1 regulates ROS-mediated cell death

DAB staining and measurement of H_2O_2 revealed an excessive accumulation of ROS in apical spikelets of *apa1331* (Fig. 5). Enhanced level of MDA and decreased relative expression level of *OsCATa, OsCATb* and *OsCATc* revealed the excessive peroxidation of fatty acids and ROS imbalance in *apa1331* (Fig. 5E). Dark staining of trypan blue and strong positive TUNEL signals revealed DNA fragmentation and cell death in *apa1331* (Fig. 5F). Previous studies have reported that the excessive occurrence of ROS causes cell death in the apical spikelets [3,14]. Enhanced ROS levels and increased PCD in the apical spikelets indicate their correlation with panicle abortion. Excessive PCD has been reported to play its role in panicle development and spikelet abortion [16,35]. Enhanced PCD is usually accompanied due to disturbance in the ROS homeostasis or external stimuli [86]. Aborted pollen grains, failure of normal microspore development and abnormal anther development have been reported due to excessive accumulation of ROS [5,67]. ROS are important signaling molecules involved in the rupture of tapetum for pollen grain development. Still, its accumulation beyond the threshold would produce oxidative stress to cellular components [87]. Hence, it is logical to refer that apical sterility in *apa1331* was caused due to excessive bursts of ROS and abnormal cell death occurrence. Our findings provide the basis

of the mechanism by which homeostasis in ROS-mediated PCD was possibly dysregulated due to the mutation in *OsSUBSrP1*. Our data support that apical spikelet abortion onset was started due to mutation in *OsSUBSrP1* and validate the potential correlation between cell death and ROS homeostasis for panicle development.

In summary, our results revealed that SUBSrP1 is essential to control the excessive outburst of ROS and programmed cell death (Fig. 10). A mutation in SUBSrP1 causes dysregulation in its function and induces abnormal cell death to apical spikelet of *apa1331*. In WT, the balanced homeostasis of ROS and antioxidants produce a normal degeneration of tapetum that is essential for normal microspore development. However, excessive ROS and abnormal cell death cause the faulty development of PMCs and defective cuticle formation in *apa1331*. Mutation in *OsSUBSrP1* results in the impairment in transferring fatty acid molecules to developing pollen that causes sterility. Defective cuticle formation and a significant decrease in wax and cutin contents cause the excessive water loss that produced aborted apical spikelet in *apa1331*. However, in WT, normal development of anther cuticle and wax saves enough water for cell viability and provides fatty acid to develop regular pollen grains. Our hypothesized model supports that SUBSrP1 is essential for maintaining ROS homeostasis by regulating wax and cutin development in rice.

Compliance with Ethics Requirements

This article does not contain any studies with human or animal subjects.

CRediT authorship contribution statement

Asif Ali: Methodology, Software, Formal analysis, Data curation, Validation, Investigation, Writing original draft. **Tingkai Wu:** Formal analysis, Methodology. **Hongyu Zhang:** Resources. **Peizhou Xu:** Validation, Data curation. **Syed Adeel Zafar:** Conceptualization, Validation, Writing review & editing. **Yongxiang Liao:**

Resources. **Xiaoqiong Chen:** Data curation. **Hao Zhou:** Software. **Yutong Liu:** Resources. **Wenming Wang:** Supervision, Writing review & editing. **Xianjun Wu:** Project administration, Funding acquisition, Visualization, Writing review & editing.

Declaration of Competing Interest

The authors declare that they have no known competing financial interests or personal relationships that could have appeared to influence the work reported in this paper.

Acknowledgments

Appendix A. Supplementary material

Supplementary data to this article can be found online at https://doi.org/10.1016/j.jare.2022.01.003.

References

[1] Zhu Z, Tan L, Fu Y, Liu F, Cai H, Xie D, et al. Genetic control of inflorescence architecture during rice domestication. Nat Commun 2013;4(1). doi: https://doi.org/10.1038/ncomms3200.

[2] Teo ZWN, Song S, Wang Y-Q, Liu J, Yu H. New insights into the regulation of inflorescence architecture. Trends Plant Sci 2014;19(3):158–65.

[3] Heng Y, Wu C, Long Yu, Luo S, Ma J, Chen J, et al. OsALMT7 maintains panicle size and grain yield in rice by mediating malate transport. Plant Cell 2018;30(4):889–906.

[4] Lu H, Dai Z, Li L, Wang J, Miao X, Shi Z. OsRAMOSA2 shapes panicle architecture through regulating pedicel length. Front Plant Sci 2017;8.

[5] Zafar SA, Patil SB, Uzair M, Fang J, Zhao J, Guo T, et al. DEGENERATED PANICLE AND PARTIAL STERILITY 1 (DPS 1) encodes a cystathionine -synthase domain containing protein required for anther cuticle and panicle development in rice. New Phytol 2020;225(1):356–75.

[6] Tanaka W, Pautler M, Jackson D, Hirano H. Grass meristems II Inflorescence architecture, flower development and meristem fate. Plant Cell Physiol 2013;54(3):313–24.

[7] Li S, Qian Q, Fu Z, Zeng D, Meng X, Kyozuka J, et al. Short panicle1 encodes a putative PTR family transporter and determines rice panicle size. Plant J 2009;58(4):592–605.

[8] Zhu K, Tang D, Yan C, Chi Z, Yu H, Chen J, et al. ERECT PANICLE2 encodes a novel protein that regulates panicle erectness in indica rice. Genetics 2010;184(2):343–50.

[9] Oikawa T, Kyozuka J. Two-step regulation of LAX PANICLE1 protein accumulation in axillary meristem formation in rice. Plant Cell 2009;21(4):1095–108.

[10] Tabuchi H, Zhang Yu, Hattori S, Omae M, Shimizu-Sato S, Oikawa T, et al. LAX PANICLE2 of rice encodes a novel nuclear protein and regulates the formation of axillary meristems. Plant Cell 2011;23(9):3276–87.

[11] Ikeda K, Nagasawa N, Nagato Y. ABERRANT PANICLE ORGANIZATION 1 temporally regulates meristem identity in rice. Dev Biol 2005;282(2):349–60.

[12] Ikedakawakatsu K, Maekawa M, Izawa T, Itoh JI, Nagato Y. ABERRANT PANICLE ORGANIZATION 2/RFL, the rice ortholog of Arabidopsis LEAFY, suppresses the transition from inflorescence meristem to floral meristem through interaction with APO1. Plant J 2012;69(1):168–80.

[13] Wang Q-L, Sun A-Z, Chen S-T, Chen L-S, Guo F-Q. SPL6 represses signalling outputs of ER stress in control of panicle cell death in rice. Nat Plants 2018;4(5):280–8.

[14] Peng Y, Hou F, Bai Q, Xu P, Liao Y, Zhang H, et al. Rice calcineurin B-like protein-interacting protein kinase 31 (OsCIPK31) is involved in the development of panicle apical spikelets. Front Plant Sci 2018;9(1661).

[15] Bai J, Zhu X, Wang Q, Zhang J, Chen H, Dong G, et al. Rice TUTOU1 encodes a suppressor of cAMP receptor-like protein that is important for actin organization and panicle development. Plant Physiol 2015;169(2):1179–91.

[16] Zhang D, Liang W, Yin C, Zong J, Gu F, Zhang D. OsC6, encoding a lipid transfer protein, is required for postmeiotic anther development in rice. Plant Physiol 2010;154(1):149–62.

[17] Yao Y, Yamamoto Y, Yoshida T, Nitta Y, Miyazaki A. Response of differentiated and degenerated spikelets to top-dressing, shading and day/night temperature treatments in rice cultivars with large panicles. Soil Sci Plant Nutr 2000;46(3):631–41.

[18] Itoh J-I, Nonomura K-I, Ikeda K, Yamaki S, Inukai Y, Yamagishi H, et al. Rice plant development: from zygote to spikelet. Plant Cell Physiol 2005;46(1):23–47.

[19] Smith AM, Stitt M. Coordination of carbon supply and plant growth. Plant, Cell Environ 2007;30(9):1126–49.

[20] Ali A, Xu P, Riaz A, Wu X. Current advances in molecular mechanisms and physiological basis of panicle degeneration in rice. Int J Mol Sci 2019;20(7):1613.

[21] Zhang D, Yuan Z, An G, Dreni L, Hu J, Kater MM. Panicle development. In: Zhang Q, Wing RA, editors. Genetics and genomics of rice. New York, NY: Springer; 2013. p. 279–95.

[22] Weng X, Wang L, Wang J, Hu Y, Du H, Xu C, et al. Grain number, plant height, and heading date7 is a central regulator of growth, development, and stress response. Plant Physiol 2014;164(2):735–47.

[23] Yi J, Moon S, Lee Y-S, Zhu Lu, Liang W, Zhang D, et al. Defective tapetum cell death 1 (DTC1) regulates ROS levels by binding to metallothionein during tapetum degeneration. Plant Physiol 2016;170(3):1611–23.

[24] Papini A, Mosti S, Brighigna L. Programmed-cell-death events during tapetum development of angiosperms. Protoplasma 1999;207(3-4):213–21.

[25] Ling S, Chen C, Wang Y, Sun X, Lu Z, Ouyang Y, et al. The mature anther-preferentially expressed genes are associated with pollen fertility, pollen germination and anther dehiscence in rice. BMC Genomics 2015;16(1):1–17.

[26] Bedinger P. The remarkable biology of pollen. Plant Cell 1992;4(8):879.

[27] Uzair M, Xu D, Schreiber L, Shi J, Liang W, Jung K-H, et al. PERSISTENT TAPETAL CELL2 is required for normal tapetal programmed cell death and pollen wall patterning. Plant Physiol 2020;182(2):962–76.

[28] Li Na, Zhang D-S, Liu H-S, Yin C-S, Li X-X, Liang W-q, et al. The rice tapetum degeneration retardation gene is required for tapetum degradation and anther development. Plant Cell 2006;18(11):2999–3014.

[29] Liu Ze, Lin S, Shi J, Yu J, Zhu Lu, Yang X, et al. Rice No Pollen 1 (NP 1) is required for anther cuticle formation and pollen exine patterning. Plant J 2017;91(2):263–77.

[30] Shi J, Tan H, Yu X-H, Liu Y, Liang W, Ranathunge K, et al. Defective pollen wall is required for anther and microspore development in rice and encodes a fatty acyl carrier protein reductase. Plant Cell 2011;23(6):2225–46.

[31] Liao Y, Bai Q, Xu P, Wu T, Guo D, Peng Y, et al. Mutation in rice abscisic acid2 results in cell death, enhanced disease-resistance, altered seed dormancy and development. Front Plant Sci 2018;9.

[32] Rang ZW, Jagadish SVK, Zhou QM, Craufurd PQ, Heuer S. Effect of high temperature and water stress on pollen germination and spikelet fertility in rice. Environ Exp Bot 2011;70(1):58–65.

[33] Zhang CX, Feng BH, Chen TT, Zhang XF, Tao LX, Fu GF. Sugars, antioxidant enzymes and IAA mediate salicylic acid to prevent rice spikelet degeneration caused by heat stress. Plant Growth Regul 2017;83(2):313–23.

[34] Nawrath C. Unraveling the complex network of cuticular structure and function. Curr Opin Plant Biol 2006;9(3):281–7.

[35] Jung K-H, Han M-J, Lee D-Y, Lee Y-S, Schreiber L, Franke R, et al. Wax-deficient anther1 is involved in cuticle and wax production in rice anther walls and is required for pollen development. Plant Cell 2006;18(11):3015–32.

[36] Zhu Lu, Shi J, Zhao G, Zhang D, Liang W. Post-meiotic deficient anther1 (PDA1) encodes an ABC transporter required for the development of anther cuticle and pollen exine in rice. J Plant Biol 2013;56(1):59–68.

[37] Chang Z, Chen Z, Yan W, Xie G, Lu J, Wang Na, et al. An ABC transporter, OsABCG26, is required for anther cuticle and pollen exine formation and pollen-pistil interactions in rice. Plant Sci 2016;253:21–30.

[38] Wu Y, Wang Y, Mi X, Shan J, Li X, Xu J, et al. The QTL GNP1 encodes GA20ox1, Which increases grain number and yield by increasing cytokinin activity in rice panicle meristems. PLOS Genetics 2016;12(10).

[39] Chen X, Zhang H, Sun H, Luo H, Zhao Li, Dong Z, et al. IRREGULAR POLLEN EXINE1 is a novel factor in anther cuticle and pollen exine formation. Plant Physiol 2017;173(1):307–25.

[40] Xu D, Shi J, Rautengarten C, Yang Li, Qian X, Uzair M, et al. Defective Pollen Wall 2 (DPW2) encodes an acyl transferase required for rice pollen development. Plant Physiol 2017;173(1):240–55.

[41] Mondol PC, Xu D, Duan L, Shi J, Wang C, Chen X, et al. Defective Pollen Wall 3 (DPW3), a novel alpha integrin-like protein, is required for pollen wall formation in rice. New Phytol 2020;225(2):807–22.

[42] Chen W, Yu X-H, Zhang K, Shi J, De Oliveira S, Schreiber L, et al. Male Sterile2 encodes a plastid-localized fatty acyl carrier protein reductase required for pollen exine development in Arabidopsis. Plant Physiol 2011;157(2):842–53.

[43] Vartapetian AB, Tuzhikov AI, Chichkova NV, Taliansky M, Wolpert TJ. A plant alternative to animal caspases: subtilisin-like proteases. Cell Death Differ 2011;18(8):1289–97.

[44] Coffeen WC, Wolpert TJ. Purification and characterization of serine proteases that exhibit caspase-like activity and are associated with programmed cell death in Avena sativa. Plant Cell 2004;16(4):857–73.

[45] Srivastava R, Liu JX, Howell SH. Proteolytic processing of a precursor protein for a growth-promoting peptide by a subtilisin serine protease in Arabidopsis. Plant J 2008;56(2):219–27.

[46] Othman R, Nuraziyan A. Fruit-specific expression of papaya subtilase gene. J Plant Physiol 2010;167(2):131–7.

[47] Zhao C, Johnson BJ, Kositsup B, Beers EP. Exploiting secondary growth in Arabidopsis. Construction of xylem and bark cDNA libraries and cloning of three xylem endopeptidases. Plant Physiol 2000;123(3):1185–96.

[48] Figueiredo A, Monteiro F, Sebastiana M. Subtilisin-like proteases in plantpathogen recognition and immune priming: a perspective. Front Plant Sci 2014;5:739.

[49] Martinez DE, Borniego ML, Battchikova N, Aro E-M, Tyystjõrvi E, GuiamÕt JJ. SASP, a Senescence-Associated Subtilisin Protease, is involved in reproductive development and determination of silique number in Arabidopsis. J Exp Bot 2015;66(1):161–74.

[50] Yoshida KT, Kuboyama T. A subtilisin-like serine protease specifically expressed in reproductive organs in rice. Sex Plant Reprod 2001;13(4): 193–9.

[51] Taylor AA, Horsch A, Rzepczyk A, Hasenkampf CA, Riggs CD. Maturation and secretion of a serine proteinase is associated with events of late microsporogenesis. Plant J 1997;12(6):1261–71.

[52] Hou F, Peng Y, Han X, Bai Q, Gu C, Sun C, et al. Identification and gene mapping of a panicle apical abortion mutant (paa1331) in rice (in Chinese). Chin Sci Bull 2018;63:3192–203.

[53] Chun Y, Fang J, Zafar SA, Shang J, Zhao J, Yuan S, et al. MINI SEED 2 (MIS2) encodes a receptor-like kinase that controls grain size and shape in rice. Rice 2020;13(1):1–17.

[54] Wu J, Yang R, Yang Z, Yao S, Zhao S, Wang Yu, et al. ROS accumulation and antiviral defence control by microRNA528 in rice. Nat Plants 2017;3(1). doi: https://doi.org/10.1038/nplants.2016.203.

[55] Adeel Zafar S, Uzair M, Ramzan Khan M, Patil SB, Fang J, Zhao J, et al. DPS1 regulates cuticle development and leaf senescence in rice. Food Energy Secur 2021;10(1). doi: https://doi.org/10.1002/fes3.v10.110.1002/fes3.273.

[56] Wilson ZA, Zhang D. From Arabidopsis to rice: pathways in pollen development. J Exp Bot 2009;60(5):1479–92.

[57] Wu T, Ali A, Wang J, Song J, Fang Y, Zhou T, et al. A homologous gene of OsREL2/ASP1, ASP-LSL regulates pleiotropic phenotype including long sterile lemma in rice. BMC Plant Biol 2021;21(1). doi: https://doi.org/10.1186/s12870-021-03163-7.

[58] Abe A, Kosugi S, Yoshida K, Natsume S, Takagi H, Kanzaki H, et al. Genome sequencing reveals agronomically important loci in rice using MutMap. Nat Biotechnol 2012;30(2):174–8.

[59] Ma X, Zhu Q, Chen Y, Liu Y-G. CRISPR/Cas9 platforms for genome editing in plants: developments and applications. Molecular Plant 2016;9(7):961–74.

[60] Toki S, Hara N, Ono K, Onodera H, Tagiri A, Oka S, et al. Early infection of scutellum tissue with Agrobacterium allows high-speed transformation of rice. Plant J 2006;47(6):969–76.

[61] Tripathi LP, Sowdhamini R. Cross genome comparisons of serine proteases in Arabidopsis and rice. BMC Genomics 2006;7(1):1–31.

[62] Kumar S, Stecher G, Li M, Knyaz C, Tamura K, Battistuzzi FU. MEGA X: molecular evolutionary genetics analysis across computing platforms. Mol Biol Evol 2018;35(6):1547–9.

[63] Li H, Durbin R. Fast and accurate short read alignment with Burrows-Wheeler transform. Bioinformatics 2009;25(14):1754–60.

[64] Consortium GO. Expansion of the Gene Ontology knowledgebase and resources. Nucleic Acids Res 2017;45(D1):D331–8.

[65] Liu J, Zhu L, Wang B, Wang H, khan I, Zhang S, et al. BnA1. CER4 and BnC1. CER4 are redundantly involved in branched primary alcohols in the cuticle wax of Brassica napus. Theor Appl Genet 2021;134(9):3051–67.

[66] Men X, Shi J, Liang W, Zhang Q, Lian G, Quan S, et al. Glycerol-3-Phosphate Acyltransferase 3 (OsGPAT3) is required for anther development and male fertility in rice. J Exp Bot 2017;68(3):513–26.

[67] Hu L, Liang W, Yin C, Cui X, Zong J, Wang X, et al. Rice MADS3 regulates ROS homeostasis during late anther development. Plant Cell 2011;23(2):515–33.

[68] Gomez JM, Jimenez AI, Olmos E, Sevilla F. Location and effects of long-term NaCl stress on superoxide dismutase and ascorbate peroxidase isoenzymes of pea (Pisum sativum cv. Puget) chloroplasts. J Exp Bot 2003;55(394):119–30.

[69] Schmidt A, Kunert KJ. Lipid peroxidation in higher plants: the role of glutathione reductase. Plant Physiol 1986;82(3):700–2.

[70] Zhu X, Yin J, Liang S, Liang R, Zhou X, Chen Z, et al. The multivesicular bodies (MVBs)-localized AAA ATPase LRD6-6 inhibits immunity and cell death likely through regulating MVBs-mediated vesicular trafficking in rice. PLOS Genetics 2016;12(9):e1006311.

[71] Wutipraditkul N, Boonkomrat S, Buaboocha T. Cloning and characterization of catalases from rice, Oryza sativa L. Biosci Biotechnol Biochem 2011;75 (10):1900–6.

[72] Ouyang S, Zhu W, Hamilton J, Lin H, Campbell M, Childs K, et al. The TIGR rice genome annotation resource: improvements and new features. Nucleic Acids Res 2007;35(Database):D883–7.

[73] Rawlings ND, Barrett AJ, Bateman A. MEROPS: the peptidase database. Nucleic Acids Res 2010;38(suppl_1):D227–33.

[74] Rautengarten C, Steinhauser D, B≈ssis D, Stintzi A, Schaller A, Kopka J, et al. Inferring hypotheses on functional relationships of genes: analysis of the Arabidopsis thaliana subtilase gene family. PLoS Comput Biol 2005;1(4):e40.

[75] Beers EP, Jones AM, Dickerman AW. The S8 serine, C1A cysteine and A1 aspartic protease families in Arabidopsis. Phytochemistry 2004;65(1):43–58.

[76] Dodson G, Wlodawer A. Catalytic triads and their relatives. Trends Biochem Sci 1998;23(9):347–52.

[77] Siezen RJ, Leunissen JAM. Subtilases: the superfamily of subtilisin-like serine proteases. Protein Sci 1997;6(3):501–23.

[78] Itzhaki H, Naveh L, Lindahl M, Cook M, Adam Z. Identification and characterization of DegP, a serine protease associated with the luminal side of the thylakoid membrane. J Biol Chem 1998;273(12):7094–8.

[79] Lin H, Yu J, Pearce SP, Zhang D, Wilson ZA. RiceAntherNet: a gene co-expression network for identifying anther and pollen development genes. Plant J 2017;92(6):1076–91.

[80] Waese J, Fan J, Pasha A, Yu H, Fucile G, Shi R, et al. ePlant: visualizing and exploring multiple levels of data for hypothesis generation in plant biology. Plant Cell 2017;29(8):1806–21.

[81] Wang X, Guan Y, Zhang Du, Dong X, Tian L, Qu LQ. A -ketoacyl-CoA synthase is involved in rice leaf cuticular wax synthesis and requires a CER2-LIKE protein as a cofactor. Plant Physiol 2017;173(2):944–55.

[82] Ibrahim S, Saleem B, Rehman N, Zafar SA, Naeem MK, Khan MR. CRISPR/Cas9 mediated disruption of Inositol Pentakisphosphate 2-Kinase 1 (TaIPK1) reduces phytic acid and improves iron and zinc accumulation in wheat grains. J Adv Res 2021. doi: https://doi.org/10.1016/j.jare.2021.07.006.

[83] JordÃ L, Coego A, Conejero V, Vera P. A genomic cluster containing four differentially regulated subtilisin-like processing protease genes is in tomato plants. J Biol Chem 1999;274(4):2360–5.

[84] Samuels L, Kunst L, Jetter R. Sealing plant surfaces: cuticular wax formation by epidermal cells. Annu Rev Plant Biol 2008;59(1):683–707.

[85] Aharoni A, Dixit S, Jetter R, Thoenes E, Van Arkel G, Pereira A. The SHINE clade of AP2 domain transcription factors activates wax biosynthesis, alters cuticle properties, and confers drought tolerance when overexpressed in Arabidopsis. Plant Cell 2004;16(9):2463–80.

[86] Mittler R, Del Pozo O, Meisel L, Lam E. Pathogen-induced programmed cell death in plants, a possible defense mechanism. Dev Genet 1997;21(4):279–89.

[87] Duan Q, Kita D, Johnson EA, Aggarwal M, Gates L, Wu H-M, et al. Reactive oxygen species mediate pollen tube rupture to release sperm for fertilization in Arabidopsis. Nat Commun 2014;5(1):1–10.